EPJ manuscript No.
(will be inserted by the editor)

Theoretical Investigations on the Stark-Zeeman Effect of the $2p\ ^2P_{3/2}$-Level in ^6Li for Perpendicularly Crossed Fields

Ewald Rößl[1], Bernhard Schnizer[2] and Maurizio Musso[3]

[1] Institut für Theoretische Physik, Technische Universität Graz, A-8010 Graz, Austria; Present adress: Philips Forschungslaboratorien, Technische Systeme Hamburg, D-22335 Hamburg, e-mail: ewald.roessl@philips.com

[2] Institut für Theoretische Physik, Technische Universität Graz, A-8010 Graz, Austria, e-mail: schnizer@itp.tu-graz.ac.at

[3] Abteilung für Physik and Biophysik, Fachbereich Molekulare Biologie, Universität Salzburg, A-5020 Salzburg e-mail: Maurizio.Musso@sbg.ac.at

Received: date / Revised version: date

Abstract. The splitting behaviour of the 2p $^2P_{3/2}$ hyperfine structure levels is investigated in ^6Li for homogeneous crossed electric and magnetic fields (Stark-Zeeman effect). This is done by diagonalizing the perturbation matrix comprising the hyperfine interaction, the electronic and nuclear magnetic interaction and the effective electric interaction obtained by transforming the quadratic Stark effect to a first order perturbation interaction. Symmetries are used to find analytic formulae for level shifts and crossing points if only one external field is present. A reflection symmetry unbroken with all three interactions present permits the decomposition of the 12×12 matrix into two 6×6 submatrices. The structure of energy eigenvalue surfaces $\epsilon_{F,M_F}(B,E)$ of the two subsystems is found by numeric diagonalization of the perturbation matrix and is displayed in the ranges $|B| < 1$ mT, $|E| < 300$ kV/cm. The total angular momentum $F = J+I$ ($J = 3/2$, electronic angular momentum, $I = 1$, nuclear spin) and the magnetic quantum number M_F provide labels for all surfaces. All crossing points of the energy surfaces have been found. Adiabatic level transfer occurring in atoms traversing a sequence of crossed magnetic and electric fields is explained. Berry phases occur for cycles around some crossing points. Their presence or absence is explained.

PACS. 03.65.Vf Berry phase – 32.60.+i Zeeman and Stark effects – 32.80.Bx Level crossing-atoms – 3150.Gh Surface crossings

1 Introduction

In the past efforts have been made to investigate the Stark-Zeeman effect of the $np\ ^2P_{3/2}$-levels of the alkalines, both experimentally by means of laser-atomic-beam spectroscopy in parallel and in crossed fields, and computationally by means of a programme which determined the splitting of the hyperfine components of the spectral lines considered, and their expected relative transition probabilities [1] - [8]. The computed data were compared with the experimental spectra with the help of fitting procedures, resulting in the determination of atomic parameters, like the hyperfine structure constants, and/or polarizabilities. This same programme was used in the laserspectroscopic study of the lithium and the sodium D-lines in strong magnetic fields up to 1 T [9], [10], i.e. strong enough to observe the influence of the fine structure levels $J = 1/2$ and $J = 3/2$ of the excited term ^{2}P on each other. As a subsequent step, the computation of the splitting of the hyperfine states M_F of an atom influenced by crossed electric and magnetic fields showed that, adiabatically changing the presence and the strength of these fields according to a well defined cycle, atoms populated in a given hyperfine level F_i before the start of the field cycle were found in another level F_f after experiencing the field cycle [5], [7], [8]. This kind of level transfer, explainable as the consequence of the presence of level crossings and anticrossings, was experimentally proved in a laserspectroscopic experiment on a beam of gallium atoms, by successfully probing the population of the levels involved [12]. However, these considerations for energy levels with the electronic angular momentum $J = 3/2$ have so far been limited to atoms with nuclear spin $I = 3/2$ as ^{23}Na, ^{69}Ga, ^{71}Ga [13] or ^{7}Li [14]. For this reason, similar investigations have been performed for ^{6}Li, which has an integer nuclear spin, $I = 1$, in order to find differences and similarities.

These have been performed by diagonalizing the perturbation matrix comprising the following three interactions (see Section 2): 1) the hyperfine interaction between the valence electron and the nucleus; 2) the interaction of the electronic and nuclear magnetic moments with the constant external magnetic field; 3) the effective electric interaction of the valence electron with the constant external electric field, developed by Schmieder [15] [16], in which the quadratic Stark effect is represented by an equivalent operator fitting the framework of first order perturbation theory. Basic theory gives the analytic form of these operators, their strengths being fixed by experimentally accessible atomic parameters. In the case of 1) these are the diagonal hyperfine structure constants A_1 and A_2, in case of 2) the electronic and nuclear gyromagnetic ratios g_J and $\hat{g}_I$, and in the case of 3) the scalar and tensor polarizabilities α_0 and α_2. In the following all the expressions for the matrix elements of these operators needed for the calculations are given and discussed as well as their symmetry properties. The eigenvalues are only approximate, since only the subspace belonging to the 2p ^{2}P$_{3/2}$ level is used. The nearest level is the other fine structure level, 2p ^{2}P$_{1/2}$, whose energy is 10050 MHz lower [17]. The magnitude of this fine structure splitting is much larger than the hyperfine shifts considered here. An analysis where

this state is included has been performed for ^{7}Li in [14] and will be published elsewhere. The corrections to the field values and energies of the crossing points do not exceed 17 %. Additional corrections may come from changes of the experimental values of the atomic constants discussed above and listed in Table.1. But all such corrections will change our results only quantitatively, but not qualitatively.

For perpendicular external fields, the only unbroken symmetry is a reflection at a plane perpendicular to the magnetic field B and parallel to the electric field E (see Section 3); it permits one to decompose the 12-dimensional function space into two orthogonal 6-dimensional subspaces, which we call the positive and the negative subsystem. The positive subsystem is characterized by the magnetic quantum numbers $M_F = 5/2, 1/2, -3/2$; the negative subsystem by $M_F = -5/2, -1/2, 3/2$. The corresponding two characteristic polynomials can be further decomposed if one of the external fields is zero. In either case, each of the polynomials separates into three polynomials, which are linear, quadratic and cubic in either B or E^2. The corresponding eigenvalues of the first and the second factor are given as analytic expressions in Section 4. The crossing points, which are very important for the topology of the level subsystem, the adiabatic level transfer and the geometric phases, are found from the resultants of these polynomials (see Section 4). There are 7 crossing points in each subsystem in the domain $|B| < 1$ mT, $0 < E < 300$ kV/cm of the B, E-plane. In case of a pure magnetic field, each subsystem possesses 5 crossing points. In case of a pure electric field there is one crossing point. An additional crossing point has both fields different from zero.

There is a qualitative difference between the systems with nuclear spin $I = 3/2$ leading to a integer total angular momentum F [8], [13] and the present system with $I = 1$ leading to a half odd integer F. Both systems decompose into two non-interacting subsystems due to the fact that the interaction mixes only those states M_F differing by $\Delta M_F = 0, \pm 2$, enabling one to catalogue them as the odd subsystem (M_F = odd) and the even subsystem (M_F = even) for $I = 3/2$ (and presumably for other one electron systems having a nucleus with half odd integer spin) and the positive and the negative subsystem for $I = 1$. The positive and the negative subsystem are very similar [14], whereas the odd and the even system exhibit several qualitative differences [7], [8], [13].

In the general case where both fields are nonzero, the energy eigenvalues $\epsilon_{F,M_F}(B, E)$ are found by numerical diagonalization of the perturbation matrix. The corresponding surfaces above the B, E-plane are plotted. The insight taken from these pictures leads to an understanding of the adiabatic level transfer (see Section 7). In a single increasing external field the phase point describing the state of the atom passes from one energy surface to another one through the crossing points (crossing); when this field decreases in the presence of a second field the gap now separating the two surfaces detains the phase point from returning to the original surface (anticrossing). The knowledge of the crossing points permits one to predict all types of behaviour of an atom in such a sequence of fields.

A crossing requires the coincidence of two eigenvalues of the Hamiltonian. In a seminal paper [18] v. Neumann and Wigner proved the following rules: *A real symmetric matrix* (as is the Hamiltonian considered here), *whose elements depend on a number of parameters* $\alpha_1, \alpha_2, \ldots, \alpha_n$, *has a double eigenvalue if* n*, the number of parameters, is at least 2.* This entails: *Terms belonging to the same irreducible representation of the unbroken symmetry do not cross under the influence of a one-parameter perturbation.* Haake [19] gives an extensive and thorough discussion of the time-reversal operator, T, as well as the connections between this and other symmetry operations and degeneracies. In our case $T^2 = -1$, since total angular momentum is a half odd integer. Haake's [19] results will be used below in several applications.

When there is a crossing of levels one is wondering whether Berry (or geometrical) phases occur in field cycles enclosing the crossing points. Such phases are indeed found, but only for some of the crossing points (see Section 8). The absence or presence of such phase changes is correlated with the structure of the energy surfaces at the crossing points. When the Taylor series of the $\epsilon_{F,M_F}(B,E)$ around a given crossing point are linear in both B and E, then a Berry phase occurs. The quadratic Stark effect introduces a quadratic dependence of $\epsilon_{F,M_F}(B,E)$ on E for the magnetic crossing points, Bp1, ..., Bp5, Bn1, ... Bp5, shown in Figs. 1, 7 and 8, thereby preventing such a phase for the corresponding field cycles.

2 The perturbation operators

In this investigation the function space is limited to the wave functions belonging to the 2p $^2P_{3/2}$ fine structure level of ^{6}Li. The nuclear spin and the total electronic angular momentum are $I = 1$ and $J = 3/2$. These angular momenta are assumed to remain good quantum numbers. Their coupling gives the total angular momentum, characterized by quantum numbers $F = 5/2, 3/2, 1/2$. So the degeneracy of the unperturbed system, which is also the dimension of our function space, is 12. The theory has been collected and discussed in [1] or [14]. The matrix elements of the perturbation operators are evaluated by the Wigner-Eckhart theorem, choosing the coupled wavefunctions $|\gamma_I \gamma_J I J F M_F\rangle$ as a basis. The radial part of the interaction is the same for all matrix elements and is absorbed into the atomic parameters (hyperfine structure constants, polarizabilities) or drops out as the magnetic interactions do not depend on the radius in our approximation. Since the quantum numbers I and J are constant within the subspace under study, they are omitted in the following. By diagonalizing the sum of the perturbation operators (= hyperfine structure operator + magnetic interaction operator + effective electric interaction operator) within this subspace of the total Hilbert space, one obtains the energy eigenvalues and the corresponding eigenvectors of the different levels. These eigenvalues give the energy shifts with respect to the energy of the unperturbed state, which is put to zero by definition. The units of the experimentally accessible atomic parameters (see Table 1) are such that the eigenvalues (ϵ_n and ϵ'_n)

are given in frequency units, i.e. in the present case in MHz. The degeneracies are totally removed (or partially in the case of the common influence of the hyperfine and the Stark interactions; this is explained in more detail below). In the following, the three perturbation operators are described separately.

2.1 Hyperfine structure interaction

The Hamiltonian of the hyperfine interaction can in general be written as a sum of scalar products of spherical tensor operators of the form

$$H_{\rm h} = \sum_{k>0} \left(\mathbf{T}^{(k)} \cdot \mathbf{M}^{(k)} \right) \ . \tag{1}$$

In equation (1) the operator $\mathbf{T}^{(k)}$ contains only the electronic, the operator $\mathbf{M}^{(k)}$ the nuclear degrees of freedom. All the nuclear momenta are regarded as given constants. Terms with even k represent the electric interaction, terms with odd k the magnetic interaction. It is sufficient to limit the sum to $k \leq 2$; the influence of the higher multipoles ($k \geq 3$) is assumed to be negligibly small. $k = 0$ is excluded, as this interaction between the electric field of a point nucleus surrounded by closed electron shells and the valence electron is already contained in the unperturbed Hamiltonian; so is the magnetic dipolar interaction between the orbital and the spin angular momentum of the valence electron (fine structure). The $k = 1$ term in eq. (1) contains the magnetic interaction between the electronic (orbital and spin) and the nuclear magnetic moments as well as the contact term describing the polarization of the nucleus by the valence electron. The $k = 2$ term takes into account the electric interaction between the nuclear and electronic quadrupole distributions. The use of the Wigner-Eckhart theorem and Racah-algebra leads to matrix elements of the form

$$\langle \gamma_I \gamma_J I J F M_F | H_{\rm h} | \gamma_I \gamma_J I J F' M'_F \rangle = \tag{2}$$
$$= \textstyle\sum_{k>0} (-1)^{I+J+F} \begin{Bmatrix} J & I & F \\ I & J & k \end{Bmatrix} \dfrac{h A_k}{\begin{pmatrix} J & k & J \\ -J & 0 & J \end{pmatrix} \begin{pmatrix} I & k & I \\ -I & 0 & I \end{pmatrix}}.$$

The atomic parameters A_k are the so-called diagonal hyperfine structure constants.

2.2 Magnetic interaction

The Hamiltonian of the interaction with the constant, external magnetic field B aligned with the z-axis is given by the energy of the atomic and nuclear magnetic dipole moments in that field:

$$H_{\rm m} = -\left(\mu_J + \mu_I\right) \mathbf{B} = \left(g_J J_z - \hat{g}_I I_z\right) \mu_B B_z. \tag{3}$$

Here μ_B is the Bohr magneton, g_J and $\hat{g}_I = g_I \ m_e/m_p$ are the electronic and nuclear gyromagnetic ratios. These atomic parameters are taken from experiment. In the same basis as above the matrix elements become

$$\langle I J F M_F | H_{\rm m} | I J F' M'_F \rangle = \tag{4}$$
$$\mu_B B_z (-1)^{F-M_F} \begin{pmatrix} F & 1 & F' \\ -M_F & 0 & M'_F \end{pmatrix} \sqrt{(2F+1)(2F'+1)} \cdot$$
$$\cdot \Big[g_J (-1)^{I+J+1+F} \sqrt{(2J+1)(J+1)J} \begin{Bmatrix} J & F & I \\ F' & J & 1 \end{Bmatrix} -$$
$$- \hat{g}_I (-1)^{I+J+1+F'} \sqrt{(2I+1)(I+1)I} \begin{Bmatrix} I & F & J \\ -F' & I & 1 \end{Bmatrix} \Big].$$

.

2.3 Effective electric interaction

In the selected basis the first order matrix elements of the Hamiltonian describing the interaction with a constant, external electric field

$$H_{\rm el} \;=\; e\,\mathbf{r}\cdot\mathbf{E} \tag{5}$$

are zero (for reasons of parity). In order to treat the second order electric interaction still in the framework of first order perturbation theory (together with the hyperfine structure and the magnetic interaction) it is useful to define an effective electric operator (which is quadratic in E). This is described in [15], [16] . The matrix elements of the operator $H_{\rm e}$ in the above basis turn out to be

$$\langle IJFM_F|H_{\rm e}|IJF'M'_F\rangle = \tag{6}$$

$$-\tfrac{1}{2}\alpha_0 E^2\delta_{FF'}\delta_{M_FM'_F} - \tfrac{1}{2}\alpha_2 E^2 Q_{FM_F,F'M'_F}$$

with α_0 the scalar polarizability, α_2 the tensor polarizability and

$$Q_{FM_F,F'M'_F} = \tag{7}$$

$$= \sqrt{\tfrac{15}{2}}\sqrt{\tfrac{(J+1)(2J+1)(2J+3)}{J(2J-1)}}\sqrt{(2F+1)(2F'+1)}\cdot$$

$$\left\{\begin{array}{ccc} F & 2 & F' \\ J & I & J \end{array}\right\}\sum_{q=-2}^{2}\sum_{\mu=-1}^{1}\sum_{\mu'=-1}^{1}\left(\begin{array}{ccc} 1 & 2 & 1 \\ \mu & -q & \mu' \end{array}\right)\cdot$$

$$(-1)^{I+J-F'+F-M_F}\left(\begin{array}{ccc} F & 2 & F' \\ M_F & q & -M'_F \end{array}\right) n_\mu n_{\mu'}.$$

$n_\mu = E_\mu/E$ are the spherical components of the unit vector giving the field direction. In the case of crossed fields, we take $\mathbf{E} = E\mathbf{e}_x$, so that $n_{\pm1} = \mp1/\sqrt{2}$, $n_0 = 0$. The exception, where $\mathbf{E} = E\mathbf{e}_z$, $n_{\pm1} = 0$, $n_0 = 1$ will be noted explicitly.

3 Fundamental symmetry properties

In the absence of external fields the fundamental rotational invariance of the hyperfine structure operator of the system leads to the natural degeneracies within the hyperfine structure levels. The operator of this interaction is also invariant against inversions and reflections. By applying external magnetic and/or electric fields the symmetries of the total perturbation Hamiltonian are reduced and the degeneracies are (partially or totally) removed.

3.1 Zeeman effect

If the magnetic field is taken to be parallel to the z-axis, the remaining symmetries of the Hamiltonian $H_{\rm h} + H_{\rm m}$ are

1. rotations around the z-axis;
2. reflections at the plane perpendicular to the z-axis, i.e. the x, y-plane.

The invariance under rotations around the field axis is obvious. In considering the reflections the spins are disregarded at first. Then the interaction is proportional to $\mathbf{B}\cdot\mathbf{L} \;=\; B\,L_z$. The symmetry operations act only on the coordinates and operators of the electrons, therefore, only on L_z in the interaction term just given. L_z is invariant against reflections at the x, y-plane only. The spin operators do not contain space or momentum operators, but the symmetry properties can be taken over. This question is treated in more detail in [20]. Rotations around a symmetry axis commute with reflections at a plane perpendicular

to this axis; the symmetry group $C_{\infty h}$ is Abelian; the irreducible representations of this group are one-dimensional; so, in general, the magnetic field removes all degeneracies.

Systems with a homogeneous magnetic field are not invariant under conventional time reversal T. Haake [19] introduces a generalization, which he calls non-conventional time reversal; it is the product of a rotation by π around an axis perpendicular to the magnetic field (e.g. the $x-$axis) times T. The corresponding Hamiltonian commutes with this operation.

3.2 Stark Effect

The electric field is taken to be aligned with the x-axis. The symmetry operations that leave the Hamiltonian $H_{\rm h}+H_{\rm e}$ unchanged are:

1. rotations around the x-axis;
2. reflections at planes containing the x-axis, as e.g. the x,y-plane.

The operator, eq.(5), is linear with respect to the coordinate(s) along the electric field direction. This explains the reflection invariance just listed. The effective electric field operator, eq.(6), is quadratic in this (or these) parallel coordinate(s). This entails the additional invariance against reflections at a plane perpendicular to the field. say the $y,z-$plane. The generators of rotations around the symmetry axis and reflections at the plane through this axis anticommute; the symmetry group $C_{\infty v}$ is non-Abelian; its faithful irreducible representations (belonging to a non-zero magnetic quantum number) are two-dimensional. The corresponding levels are still at least two-fold degenerate (Kramer's degeneracy, [19]).

3.3 Perpendicular Stark-Zeeman effect

By applying both fields simultaneously, only the symmetry operations common to both interactions remain symmetries of the system. These are only the *reflection at the x,y-plane*. It is easy to show that this remaining symmetry is responsible for a very important selection rule (see [8], [13], [14], [20]) for the matrix elements of the total perturbation Hamiltonian $H_p = H_h + H_m + H_e$:

$$\langle IJFM_F|H_{\rm p}|IJF'M'_F\rangle = \\ = \begin{cases} 0 \text{ for } M_F - M'_F = \text{odd} \\ \neq 0 \text{ for } M_F - M'_F = \text{even} \end{cases}. \qquad (8)$$

This rule separates the $2{\rm p}\ ^2{\rm P}_{3/2}$ level system into two non-interacting subsystems (similarly as in ^{23}Na, ^{69}Ga, ^{71}Ga [8] and ^{7}Li, [14]):

$$\text{positive subsystem:} \quad M_F = \left\{\frac{5}{2}, \quad \frac{1}{2}, \quad -\frac{3}{2}\right\}$$
$$\text{negative subsystem:} \quad M_F = \left\{\frac{3}{2}, \quad -\frac{1}{2}, \quad -\frac{5}{2}\right\}.$$

The subspace spanned by the six vectors $|IJFM_F\rangle$ with values $M_F = \{5/2, 1/2, -3/2\}$ is called the *positive subsystem*. The six vectors $M_F = \{3/2, -1/2, -5/2\}$ are the basis of the *negative subsystem*. These names, which are chosen somewhat arbitrarily, result from the fact that a division modulo 4 of the numerators of the quantum numbers M_F gives +1 for the first set and -1 for the second set. The positive and the negative subsystems in ^{6}Li are more profoundly interrelated than the odd and even subsystems of, for example, ^{23}Na or ^{7}Li ([8], [13], [14]). In fact,

the energy shifts of one subsystems are intimately related to corresponding shifts of the other subsystem. From the formulae for the matrix elements of the perturbation operators in the decoupled basis $|IJM_IM_J\rangle$ (common eigenvectors of the operators I^2, J^2, I_z and J_z) given in [1] or [14] it is straightforward to verify the following relations

$$\langle IJ(-M_I)(-M_J)|H_{\rm h}|IJ(-M_I')(-M_J')\rangle = \\ = \langle IJM_IM_J|H_{\rm h}|IJM_I'M_J'\rangle \tag{9}$$

$$\langle IJ(-M_I)(-M_J)|H_{\rm m}|IJ(-M_I')(-M_J')\rangle = \tag{10}$$
$$= \left[g_j(-M_J) - \hat{g}_I(-M_I)\right]\mu_B B_z \cdot \delta_{(-M_I)(-M_I')}\delta_{(-M_J)(-M_J')} \\ = -\left(g_J M_J - \hat{g}_I M_I\right)\mu_B B_z \delta_{M_I M_I'}\delta_{M_J M_J'} = \\ = -\langle IJM_IM_J|H_{\rm m}|IJM_I'M_J'\rangle.$$

$$\langle IJ(-M_I)(-M_J)|H_{\rm e}|IJ(-M_I')(-M_J')\rangle = \\ = \langle IJM_IM_J|H_{\rm e}|IJM_I'M_J'\rangle. \tag{11}$$

By noting that the two eigenvectors $|IJM_IM_J\rangle$ and $|IJ(-M_I)(-M_J)\rangle$ always belong to different subsystems (a result that is no longer valid for atoms with half odd integer nuclear spin such as ^{23}Na, ^{69}Ga, ^{71}Ga or ^{7}Li) one is led to identical matrix representations provided that the magnetic field is reversed (which fact is designated by the minus sign in front of B at the r.h.s of equation 12):

$$\epsilon_i^p(B,E) \;=\; \epsilon_i^n(-B,E) \tag{12}$$

Here the superscripts p and n denote the positive and the negative subsystems, whereas the subscript $i = 1, 2, .., 6$ labels the eigenvalues.

Hamiltonians containing a magnetic field are not invariant under time reversal T. Each of the three parts of the perturbation Hamiltonian is invariant under Haake's [19] unconventional time reversal described at the end of subsection 3.1. The eigenvectors belonging to the positive and the negative subsystem are also eigenvectors of this operation and assume opposite signs.

4 Pure Zeeman and Stark splittings

4.1 Pure Zeeman effect

The magnetic field removes all natural degeneracies (see Fig.1). At first we investigate the positive subsystem. Since eigenvectors belonging to different magnetic quantum numbers M_F are orthogonal, the matrix of the Hamiltonian $H_{\rm h} + H_{\rm m}$ reduces to a 1×1 ($M_F = 5/2; F = 5/2$), a 2×2 ($M_F = -3/2; F = 5/2, 3/2$), and a 3×3 submatrix ($M_F = 1/2; F = 5/2, 3/2, 1/2$) [20]. Therefore, the characteristic polynomial decomposes into 3 polynomials of order 1, 2 and 3. The roots of the first two polynomials are easily found:

$$\epsilon = \frac{1}{4}(6a+b) - \mu_B B(\hat{g}_I - \frac{3}{2}g_J) \tag{13}$$

for $M_F = 5/2; F = 5/2$ and

$$\epsilon = \frac{1}{8}\left(2a - 3b + 4\mu_B B(\hat{g}_I - 2g_J) \;\mp\sqrt{X}\right) \tag{14}$$
$$X = 25(2a+b)^2 \; + \\ + 8\mu_B B(\hat{g}_I + g_J)(2a + b + 2\mu_B B(\hat{g}_I + g_J))$$

for $M_F = -3/2; F = 5/2, 3/2$. Instead of the diagonal hyperfine structure constants A_k appearing in eq. (2) the traditionally used hyperfine structure constants a,b ... are

employed:

$$\begin{aligned} A_1 &= IJa, \\ A_2 &= \tfrac{1}{4}b. \end{aligned} \tag{15}$$

Planck's constant h in equation (15) is omitted since from now on we choose to measure energies in MHz (s. Table 1).

For the 3×3 submatrix we provide the matrices of the hyperfine structure and the magnetic perturbation operators (ordering of basis states $|FM_F\rangle = |\frac{5}{2}\,\frac{1}{2}\rangle; |\frac{3}{2}\,\frac{1}{2}\rangle; |\frac{1}{2}\,\frac{1}{2}\rangle$):

$$\begin{aligned} H_{\mathrm{h}}^{M_F=1/2} + H_{\mathrm{m}}^{M_F=1/2} \;&= \\ = \begin{pmatrix} \frac{1}{4}(6a+b) & 0 & 0 \\ 0 & -a-b & 0 \\ 0 & 0 & \frac{5}{4}(-2a+b) \end{pmatrix} &+ \mu_B B \times \\ \times \begin{pmatrix} \frac{1}{10}(-2\hat{g}_I + 3g_J) & -\frac{3}{5}(\hat{g}_I + g_J) & 0 \\ -\frac{3}{5}(\hat{g}_I + g_J) & \frac{1}{30}(-4\hat{g}_I + 11g_J) & -\frac{1}{3}\sqrt{5}(\hat{g}_I + g_J) \\ 0 & -\frac{1}{3}\sqrt{5}(\hat{g}_I + g_J) & \frac{1}{6}(2\hat{g}_I + 5g_J) \end{pmatrix} &. \end{aligned} \tag{16}$$

The energy eigenvalues and corresponding eigenvectors are labeled uniquely by F and M_F for all field strengths under consideration ($|B| \leq 1$ mT). For small field strengths, each eigenvector coincides approximately with one of the corresponding basis vectors $|IJFM_F\rangle$. For larger values of B the admixtures may be substantial or dominating, but we can retain the labels assigned for small magnetic field strengths. By calculating the overlaps of eigenvectors belonging to slightly different B values, it is possible to continue the labels also to higher B values, even though, for large B values, the decoupled basis vectors $|IJM_IM_J\rangle$ match the real eigenvectors increasingly better. These labels, too, are shown in Fig. 1.

For some field values two curves cross at crossing points labelled Bpn. There we have an accidental degeneracy. These crossing points play an important role in level crossings. The curves $\epsilon_i^p(B, E = 0)$ shown in Fig. (1) obey the J.v.Neumann-Wigner rule quoted in the Introduction: curves belonging to the same value of F do not cross. In view of the symmetry relation (12) the diagram for the negative subsystem is obtained from that for the positive subsystem by changing the signs of the magnetic field B and of all the magnetic quantum numbers. Also the crossing points Bnn are found in this way. Analytic expressions for the corresponding field values and energies for all these crossing points can be found, in principle. But the corresponding expressions are too involved to be given here. Numerical values for all the crossing points are given in Table 2. Crossing points at $B = 0$ are disregarded.

The characteristic polynomials corresponding to eqs.(13) - (16) with an indeterminate ϵ are denoted as $c_{m1}(\epsilon)$, $c_{m2}(\epsilon)$ and $c_{m3}(\epsilon)$. Their product gives the characteristic polynomial of the total matrix. Crossing points are obtained either from a double zero of such a polynomial or from a common zero of two of these polynomials. The first type of zeros is found by computing the resultant of $c_{m2}(\epsilon)$ (or $c_{m3}(\epsilon)$) and its derivative, which is denoted as r_{m22} (or r_{m33}). A zero common to $c_{mj}(\epsilon)$ and $c_{mk}(\epsilon)$ is found from the resultant of these two polynomials denoted as r_{mjk}. All these resultants are polynomials in B; their zeros give the field values of the wanted crossing points as long as these values are real and in the range under consideration. r_{m12} gives for the crossing points Bp3 and

Bn3:

$$B_{Bp3,Bn3} = \pm \frac{(2\hat{g}_I - 3g_J)\,(2a+b)}{2\,\mu_B\,(\hat{g}_I - 3g_J)\,(\hat{g}_I - g_J)}. \qquad (17)$$

Their common energy value is found by inserting the above expression (with the positive sign) into (13):

$$\epsilon_{Bp3,Bn3} = \frac{1}{4}\left[6a + b - \frac{(2\hat{g}_I - 3g_J)^2\,(2a+b)}{(\hat{g}_I - 3g_J)\,(\hat{g}_I - g_J)}\right]. \qquad (18)$$

r_{m13} gives for the crossing points Bp4 and Bn4 the following field value:

$$B_{Bp4,Bn4} \;=\; \mp\frac{1}{N_4\;\mu_B}\left(Z_4 \;+\; \sqrt{S_4}\right). \qquad (19)$$

The corresponding energy is:

$$\epsilon_{Bp4,Bn4} \;=\; \frac{1}{2N_4}\Big(Y_4 \;+\; (2\hat{g}_I - 3g_J)\;\sqrt{S_4}\Big) \qquad (20)$$

with the following abbreviations:

$$N_4 = 8\,\hat{g}_I\;(\hat{g}_I - g_J)\;g_J\;;$$

$$Z_4 = 4\,a\,\hat{g}_I^2 + b\,\hat{g}_I^2 - 16\,a\,\hat{g}_I\,g_J + 6\,a\,{g_J}^2\;;$$

$$Y_4 = 8\,a\,\hat{g}_I^3 + 2\,b\,\hat{g}_I^3 - 20\,a\,\hat{g}_I^2\,g_J + b\,\hat{g}_I^2\,g_J + 36\,a\,\hat{g}_I\,{g_J}^2 - \\ - 4\,b\,\hat{g}_I\,{g_J}^2 - 18\,a\,{g_J}^3\;;$$

$$S_4 = (4\,a+b)^2\,\hat{g}_I^4 - 16\,b^2\,\hat{g}_I^3\,g_J + \;24\;(2\,a-b)\;b\,\hat{g}_I\,{g_J}^3 \\ - 4\;\left(4\,a^2 + 17\,a\,b - 10\,b^2\right)\;\hat{g}_I^2\,{g_J}^2 + 36\,a^2\,{g_J}^4\;.$$

r_{m23} is B^2 times a fourth order polynomial in B. The latter yields the field values for the crossing points Bp1, Bp2 and Bp5 as well as those of the corresponding crossing points Bn1, Bn2 and Bn5. The values obtained by inserting the values of the atomic parameters are given in Table 2.

4.2 Pure Stark Effect

At first we investigate the Stark effect for an electric field aligned with the z-axis as quantization axis (note that in the case of a pure Stark effect the energy shifts as functions of E^2 are independent of the field direction). The effective electric Hamiltonian is composed of two terms governed by the scalar and the tensorial polarizabilities α_0 and α_2, respectively. The term containing α_0 is proportional to the identity operator; it does not determine the field values at which crossings occur, since its influence on the energy levels is a global shift, quadratic in E, towards lower energies, not influencing energy differences. Although the effect is much stronger in magnitude than the effect caused by the term containing α_2, it is possible to diagonalize the Hamiltonian for zero α_0 to get the eigenvalues ϵ'_n related to the 'true' energy corrections ϵ_n by

$$\epsilon'_n = \epsilon_n + \frac{1}{2}\alpha_0 E^2. \qquad (21)$$

Using the eigenvalues ϵ'_n instead of ϵ_n has the advantage of a more comprehensive splitting diagram.

For the electric field aligned with the z-axis, the matrix representing the sum of the hyperfine structure and the effective electric perturbation operators $H_{\rm h} + H_{\rm e}$ can be reduced in the basis $|IJFM_F\rangle$) to a 1×1 ($M_F = 5/2; F = 5/2$), a 2×2 ($M_F = -3/2; F = 5/2, 3/2$) and a 3×3 submatrix ($M_F = 1/2; F = 5/2, 3/2, 1/2$). The roots of the characteristic polynomials are

$$\epsilon = \frac{1}{4}(6a+b) - \frac{1}{2}E^2(\alpha_0 + \alpha_2) \qquad (22)$$

for $M_F = 5/2; F = 5/2$ and

$$\epsilon = \tfrac{1}{8}\left(2a - 3b - 4\alpha_0 E^2 + \right.$$
$$\left. \mp\sqrt{16\alpha_2^2 E^4 + 8\alpha_2 E^2(2a+b) + 25(2a+b)^2}\right) \quad (23)$$

for $M_F = -3/2; F = 5/2, 3/2$. Again only the 3×3 submatrix of the effective electric perturbation operator (basis states ordered as $|FM_F\rangle = |\frac{5}{2}\,\frac{1}{2}\rangle; |\frac{3}{2}\,\frac{1}{2}\rangle; |\frac{1}{2}\,\frac{1}{2}\rangle$) is presented (since the same basis is used as in the case of the pure Zeeman effect, the submatrix of the hyperfine structure operator is the same as in eq.(16)):

$$H_{\rm e}^{M_F=1/2} = \quad (24)$$
$$E^2 \begin{pmatrix} \frac{1}{10}(-5\alpha_0 + 4\alpha_2) & \frac{\alpha_2}{5} & -\frac{\alpha_2}{2\sqrt{5}} \\ \frac{\alpha_2}{5} & \frac{1}{10}(-5\alpha_0 + \alpha_2) & \frac{\alpha_2}{\sqrt{5}} \\ -\frac{\alpha_2}{2\sqrt{5}} & \frac{\alpha_2}{\sqrt{5}} & -\frac{\alpha_0}{2} \end{pmatrix}.$$

Fig.2 shows this effect for the positive subsystem. There is a crossing point in each system for positive electric field; we call them Ep1 and En1. They result from the intersection of two levels belonging to the multiplet $F = 3/2$. This is at variance with the J.v. Neumann-Wigner rules quoted near the end of the Introduction. The explanation is: This rule has been derived under the presupposition that there are no more relations between the matrix elements except that the matrix is real symmetric. We surmise that this condition is violated on a curve passing through the points Ep1, En1 respectively. This will be the subject of a future investigation on the dynamical symmetry groups of this problem. These curves have been found in ^{23}Na and discussed by Heubrandtner [8]. In addition, a detailed investigation showed that the two-level approximation applied in [18] and many textbooks on quantum mechanics for the discussion of avoided crossings fails in this case. Indeed any approximation using less than 6 basis states is inadequate. Since the level shifts are quadratic in E, there are corresponding crossing points for negative electric field values. Taking an electric field aligned with the x-axis and separating the system of curves into the two aforementioned subsystems shows that the latter have the same Stark effect (cf. again eq. (11)). So we get the same curves as in Fig.2. But the quantum numbers assigned to these curves differ from those given in the figure.

The field value and energy of each of these electric crossing points can be found in the same way as described at the end of subsection 4.1. Characteristic polynomials $c_{e1}(\epsilon)$, $c_{e2}(\epsilon)$ and $c_{e3}(\epsilon)$ are set up (the matrix given in eq.(24) must be augmented by the first one of eq.(16) for the computation of $c_{e3}(\epsilon)$) and the resultants r_{ejk} are evaluated. The resultant r_{e23} is proportional to E^2 times a linear polynomial in E^2. This gives the field strength of the single crossing point of both systems:

$$E_{p1} = E_{n1} = \pm\frac{1}{2}\frac{\sqrt{-(2a-3b)(4a-b)(2a+b)}}{\sqrt{2a(2a-b)\ \alpha_2}}; \quad (25)$$

the corresponding energy is

$$\epsilon_{Ep1} = \epsilon_{En1} = \frac{1}{8}(2a-3b) \quad (26)$$
$$- \frac{(2a+b)(20a^2-12ab+3b^2)}{16a(2a-b)}$$
$$+ \frac{(2a-3b)(4a-b)(2a+b)\ \alpha_0}{16a(2a-b)\ \alpha_2}.$$

5 Perpendicular Stark-Zeeman effect - energy surfaces

By diagonalizing the sum of all three perturbation operators one obtains the energy eigenvalues ϵ'_n as functions of the field values B and E. Drawing the eigenvalues ϵ'_n as functions of the field values B and E gives two systems of 6 surfaces each. The quantities ϵ'_n are the eigenvalues of the operator $H_{\rm h} + H_{\rm m} + H_{\rm e}$ for $\alpha_0 \equiv 0$, which are related to the energy eigenvalues of the total Hamiltonian (including α_0) by eq. (21). For the computation of the eigenvalues the experimental values listed in Table 1 have been assigned to the atomic parameters, whereby assuming these values to be as accurate as the computational precision used.

Figs. 3-6 provide two different views of these surfaces for positive magnetic (and electric) field values and for both subsystems. For negative values of B (i.e. for the magnetic field direction reversed) the surfaces of one system go over into those of the other for positive B; this corresponds to a time reversal, so the sign of M_F changes, too. For small but finite values of the magnetic field strength and zero electric field, the quantum numbers F and M_F are good quantum numbers, therefore they distinctively name the eigenvectors. Each eigenvector and the corresponding energy eigenvalue, which gives one of the energy surfaces, is paired over the whole area of the B, E-plane under study. These pairs of quantum numbers label the surfaces in Figs. 3 and 5. In general, the connectedness of these energy surfaces is determined by the anticrossing always occurring when both fields, B and E, are different from zero and not parallel to each other [6], [18]. Then the ordering of the surfaces stays the same. This is an advantage in the numerical treatment since the labels can be assigned just by ordering the eigenvalues according to their values. The energy surfaces are smoothly connected except for the section $B = 0$ or $E = 0$ and the crossing points. If there is only one field present and if this changes continuously, crossing occurs. This entails that spikes protrude from one surface and intrude into one or several other surfaces in the vertical planes $E = 0$ and $B = 0$. This is visible more clearly in the colored versions of Figs. 3 to 6 (presented in the Electronic-only material and at our website [30]) by the edges having colors different from those of the surfaces they bound.

6 Crossing points

Crossing points are common points of two energy surfaces. These are the crossing points Bpn and Bnn found in the pure Zeeman effect and the crossing points Ep1 and En1 found from the pure Stark effect. There are additional crossing points where both fields are different from zero (called BE-crossing points). All crossing points in the $B, E-$plane are shown in Figs.7 and 8. The fact that these points of accidental degeneracy do definitely not appear along lines (in the B, E-plane) reinforces also in this context the term crossing point.

Two different methods have been used to locate points of accidental degeneracy. For the magnetic and electric crossing points, numerical root finding algorithms have

been used after sketching the energy variations graphically. The application of similar methods to the BE-crossing points did not produce satisfactory results since the root finding methods often failed. These difficulties result from the extremely slow approach of the two biconical energy surfaces in the vicinity of these crossing points. The most powerful method in this case was a method using Berry phases developed by Heubrandtner: the evolution of the eigenvectors is followed using overlap calculations along closed curves enclosing those areas to be checked for a crossing point within the plane of the field parameters; the comparison of the transported eigenvectors to the original ones shows in some cases a change in sign of some pairs of vectors. These changes can be interpreted as the appearance of geometric phases (Berry phases, which are treated in more detail in section 8). Only a real phase factor (= - 1) turns up here, since all perturbation matrices are real and symmetric. It was possible to locate the crossing points with increasing accuracy by shrinking the curves without loosing the change in sign. This method, however, has its limits, as not all crossing points show Berry phases.

The appearance of Berry phases (for certain crossing points) is closely related to the form of the energy surfaces in the neighborhood of these points [21]. Berry phases are observed only when the Taylor series expansion of the function $\epsilon(B, E)$ developed around the field values of the crossing point under study has terms linear in both B and E. Then the energy surfaces appear to form a bicone whose vertex is the crossing point. Fig. 9 illustrates this behavior for the crossing point Ep1. In the neighbourhood of the magnetic crossing points the energy values of the crossing levels depend on B and E^2; therefore the energy surfaces do not resemble to a bicone, even not to a conic section. A field cycle around such a crossing point does not lead to a Berry phase (cf. Fig. 10 for the crossing point Bp1).

7 Adiabatic hyperfine level transfer

Adiabatic hyperfine level transfers similar to those described in [5], explained in [7],[8], [13] and observed in [12] occur in ^{6}Li, too [14]. By performing adiabatic variations of the external electric and magnetic fields, starting and ending at zero field values, it is possible to achieve a level transfer; i.e. the atom's angular momentum and energy may change while the atom traverses a sequence of crossed partially overlapping static fields. In the atom's proper system the fields either vary linearly with time or stay constant, as indicated in Fig. 12 below the curves representing the energy levels. In this context adiabaticity means that the time intervals during which the field variations take place are large as compared to the times given by the reciprocals of the Bohr frequencies involved. The fact that the combination of pairs of crossing and anticrossing points is a prerequisite for observing adiabatic hyperfine level transfer is confirmed once more.

This combination of crossings and anticrossings leading to a level transfer is best understood by looking at an example where the field values and their increments are such that the phase point traverses only one crossing point, say Bn1, Fig. 11, which is an enlarged section of

the system of energy surfaces shown in Fig. 6. As long as (from the atom's point of view) $E = 0$ and B increases from a value just below B_{Bn1} to a value just beyond B_{Bn1} (cf. Fig. 8), the phase point passes from the energy surface $(F,\ M_F) = (5/2,\ 3/2)$ through the crossing point to the surface $(3/2,\ -1/2)$. The ongoing electric field leads the phase point on the latter surface away from the (vertical) plane $E = 0$ into domains where both fields are nonzero. When B decreases towards its initial value the phase point now finds a gap separating the two surfaces. It therefore cannot return to the original energy surface and quantum numbers. The same game is played for cycles with higher magnetic field strength, with the difference that the phase point may traverse several crossing points. Thus all level transfers are completely understood as soon as the system of energy surfaces with all crossing points is known. Similar considerations apply to the electric crossing points.

The preceding description by the motion of the phase point on energy surfaces is still too "classical". From the quantum mechanical point of view transition probabilities for adiabatic changes of the external fields must be considered. This has been started in [8] and studied extensively by Pfleger [21] for ^{23}Na. We believe that their results can be taken over for the other elements and also for ^{6}Li. Roughly speaking, the crossing points can be divided into two classes. The first one contains those points, in whose neighbourhood the energy functions $\epsilon'_n(B, E)$ of the levels concerned are linear in both B and E, and this neighbourhood has the shape of a bicone (s. Fig. 9, 11); all the electric crossing points of ^{6}Li and all the BE-crossing points belong to this class. Simultaneous changes of both external fields correspond to trajectories in the B, E-plane. For such trajectories passing through a crossing point of this kind the crossing probabilities are nearly the same, independent of the direction of the trajectory. On the contrary, for most of the magnetic crossing points, which make up the second class, the crossing probabilities depend strongly on the direction of the trajectory: on the one hand they are nearly unity for trajectories traversing the crossing point in the magnetic direction, i.e. if B increases (or decreases) while $E = 0$; on the other hand the crossing probability is very small if the trajectory traverses the crossing point along the electric field direction, i.e. if $B = B_{Bpn}$ or $B = B_{Bnn}$ while E changes from negative to positive values or vice versa. In ^{23}Na this picture shows some individual variations so that the true situation is less clear-cut than the description just given.

8 Berry Phases

If at least two external parameters of a system (in our case the magnetic field B and the electric field E) adiabatically pass through a closed cycle (so that at the end they have the same values as at the beginning), the wave function may not have the same value at the end which it had at the start, though the quantum numbers and energy may be the same. This change of the wave function is a phase $e^{i\gamma}$, where, in general, γ may assume any value. This geometric or Berry phase and its occurrence in different physical systems is reviewed in [22], in which Berry's papers are

also contained. An introduction into the subject is given in [23] or [24].

Herzberg and Longuet-Higgins [25] dealt with energy surfaces in polyatomic molecules already before Berry, and investigated the sign of the wavefunction in a two-level model. In this case the Hamiltonian may be represented as a real symmetric matrix with real eigenvectors. An eigenvector changes its sign if the two external parameters (there the relative positions of the nuclei) pass through a closed cycle around a crossing point of the energy surfaces. Heubrandtner detected that the same applies to the Stark-Zeeman effect for *crossed* fields. The theory of [25] may be adapted to a two-level approximation of the systems considered here. In a corresponding adiabatic treatment of an isolated diatomic molecule there is only one external parameter. If such a molecule is located in a homogenous magnetic field, then this system depends on two more external parameters, namely the field strength and the axis between the molecular and the field axis. For constant magnetic field the energy surfaces have biconical crossing points [26].

Here this phase change does not occur for each crossing point. In fact, only the eigenvectors of those levels change sign, whose energy surfaces meet at an electric or a BE crossing point, for trajectories passing around it. These crossing points (marked by circles in Figs.7 and 8) are exactly those points, in whose neighbourhood the energy functions $\epsilon'_n(B,E)$ of the levels concerned are linear in both B and E, so that the energy surfaces are connected in a bicone.

This change in sign has also been established by numerical investigations of the positive and the negative system. The program developed to perform the "analytic continuation" of the eigenvectors for changing external fields was modified: after it has found the related eigenvectors by evaluating the overlap, it ensures that the largest components of two related eigenvectors have the same sign. So it was possible to check the phase of all eigenvectors while the external fields B and E pass through a closed cycle. The corresponding trajectory is a rectangle in the $B,E-$plane. This program was again extended so that it used this property to locate unknown crossing points (s. 2^{nd} paragraph of section 6). It remains still a challenge to devise an experiment capable of detecting this phase change directly.

9 Conclusions

The splitting behaviour of the 2p $^2\mathrm{P}_{3/2}$ hyperfine structure levels in ^{6}Li for homogeneous crossed electric (E) and magnetic fields (B) has been investigated by analytical and numerical methods and the structure of the energy surfaces (i.e. frequency shifts) has been obtained from the eigenvalues $\epsilon_{F,M_F}(B,E)$ inside the domain $|B| < 1$ mT, $0 < E < 300$ kV/cm of the B,E-plane . For these field values the hyperfine, the Stark and the Zeeman interactions are of about the same strength. It has been found that:

1. If the two fields are perpendicular, the system of levels decomposes into two non-interacting subsystems

due to the remaining symmetry under reflection at a plane perpendicular to the magnetic field direction and parallel to the electric field direction. One subsystem changes into the other one under time reversal.

2. There are 7 crossing points in each subsystem; 5 with $B \neq 0$ and $E = 0$ (magnetic crossing points); 1 with $E \neq 0$ and $B = 0$ (electric crossing point); 1 with $E \neq 0$ and $B \neq 0$ (BE-crossing point).
3. The structure of the energy surfaces gives complete insight into the level transfer behaviour of the system.
4. Berry phases with a value $\pm\pi$ occur for field cycles enclosing a crossing point with linear field dependence (here the electric and BE-crossing points).

The researches presented were stimulated by experimental investigations performed in the group of L.Windholz. He provided the impetus and the experimental data, without which these investigations would not have been possible. The authors also profited from the original, clarifying results and programs of Th. Heubrandtner, which he shared generously. B.S. is obliged to B. Thaller for helpful remarks in the initial phase of this line of research. Thanks go to the anonymous referee(s) for hinting to important references and suggesting improvements.

References

1. M. E. Musso, Dr.techn.Dissertation, Technische Universität Graz, 1990.
2. M. E. Musso, Z. Phys. D **24**, 203 (1992).
3. L. Windholz, M. E. Musso, Z. Phys. D **27**, 229 (1993).
4. L. Windholz, M. E. Musso, Z. Phys. D **29**, 7 (1994).
5. M. E. Musso, L. Windholz, Z. Phys. D **30**, 13 (1994).
6. M. E. Musso, L. Windholz, S. Fischler, Z. Phys. D **33**, 239 (1995).
7. Th. Heubrandtner, B. Schnizer,M. E. Musso, L. Windholz, in: *Abstracts, 28-th EGAS Conference, Graz, 1996* edited by L. Windholz, (europhysics conference abstracts 20 D), p.189.
8. Th. Heubrandtner, Diploma Thesis, Technische Universität Graz, 1996.
9. L. Windholz, H. Jäger, M. Musso, and G. Zerza, Z. Phys. D **16**, 41 (1990)
10. Ch. H. Umfer, Diploma Thesis, Technische Universität Graz, 1992.
11. C. Umfer, L. Windholz, and M. Musso, Z. Phys. D **25**, 23 (1992).
12. L. Windholz, C. Krenn, G. Gwehenberger, M. Musso, B. Schnizer, Phys. Rev. Lett. **77**, 2190 (1996).
13. Th. Heubrandtner, B. Schnizer, M. Musso (unpublished)
14. E. Rößl, Diploma Thesis, Technical University Graz, 1999.
15. R. W. Schmieder, Am. J. Phys. **40**, 297 (1972).
16. R. W. Schmieder, IBM Research Report RW-118, 1969.
17. L. Windholz, Appl. Phys. B **60**, 573 (1995).
18. J.v. Neumann, E. Wigner, Phys.Z. **30**, 467 (1929)
19. F. Haake, *Quantum Signatures of Chaos*, (Springer, 2001).
20. R. Brandl, Diploma Thesis, Technische Universität Graz, 1999.
21. M. Pfleger, Diploma Thesis, Technische Universität Graz, 1999.
22. A. Shapere, F. Wilczek, *Geometric phases in physics* (World Scientific, Singapore, 1989).
23. J. Hamilton, *Aharonov-Bohm and other phenomena* (Springer, Berlin, 1997).

24. A. Bohm, A. Mostafazadeh, H. Koizumi, Q. Niu, J. Zwanziger, *The geometric phase in quantum systems* (Springer, Berlin, 2003).

25. G. Herzberg, H. C. Longuet-Higgins, Disc. Farad. Soc. **35**, 77 (1963). Reprinted in [22], p.74.

26. F. Schmelcher, C. Cederbaum, Phys.Rev. A **41**, 4936 (1990)

27. H. Orth, R. Veit, H. Ackermann, E. W. Otten in *Abstracts of Contributed Papers, ICAP, Heidelberg, 1981*, edited by J. Kowalski, H. G. Weber.

28. L. Windholz, M. E. Musso, G. Zerza, H. Jäger, Phys. Rev. A **46**, 5812 (1992).

29. E. Arimondo, M. Inguscio, P. Violino, Rev. Mod. Phys. **49** (1), 31 (1977).

30. The webpage: http://www.itp.tu-graz.ac.at/ ∼schnizer/Th_Atomic_Spectroscopy/ contains colored versions of the figures and refs. [8], [14], [20]. It is planned to post further reports and programs.

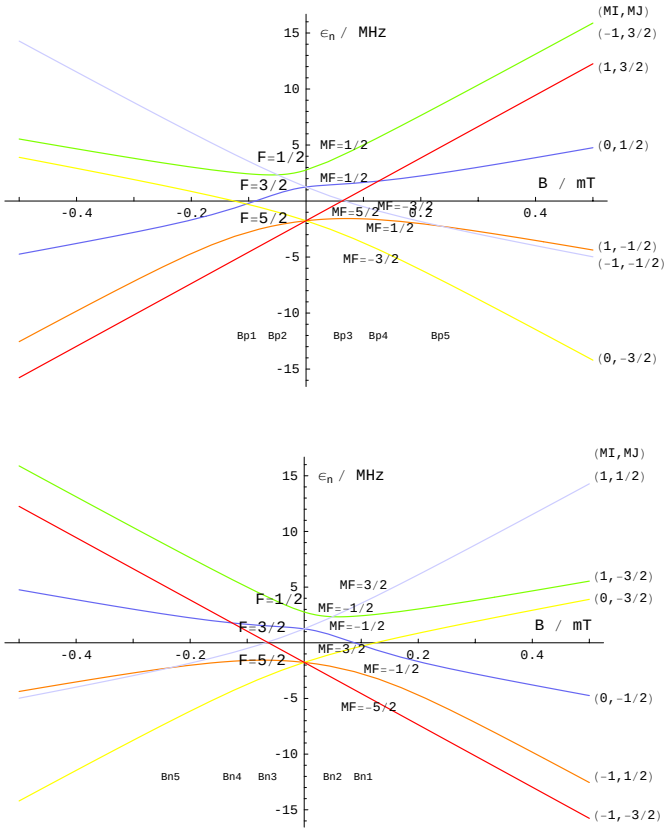

Fig. 1. Upper picture: Splitting of the 2p $^2\mathrm{P}_{\frac{3}{2}}$ hyperfine energy levels ϵ_n of ^{6}Li in the positive subsystem due to the Zeeman effect. The values of the atomic parameters used are given in Table 1 of the paper. There are five crossing points, which do not show a Berry phase; their labels (Bp1,. . . , Bp5) are located just below each one in the line at $\epsilon'_n = -12$MHz.

Lower picture: The same for the negative system with the crossing points: (Bn1,. . . , Bn5)

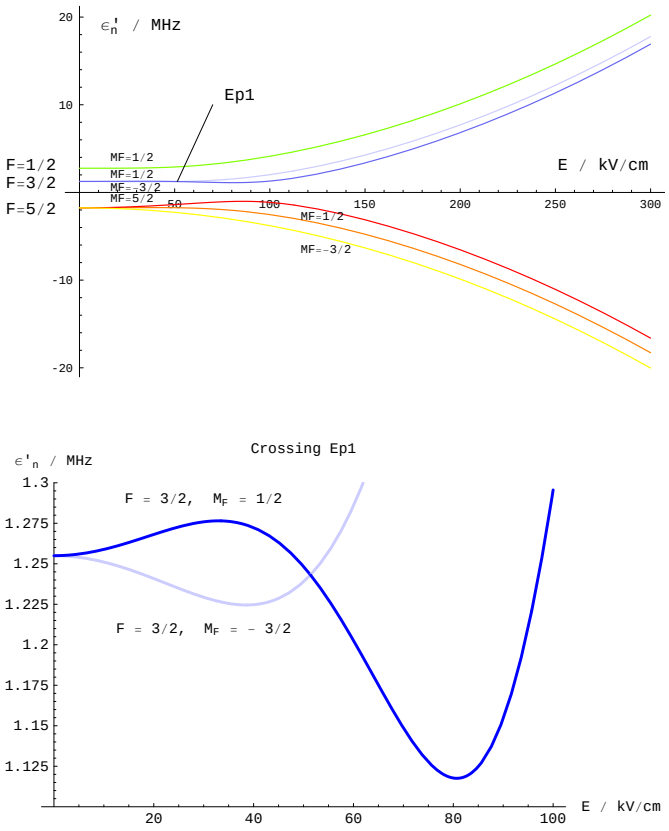

Fig. 2. Upper picture: Splitting of the 2p ^{2}P$_{\frac{3}{2}}$ hyperfine energy levels ϵ'_n of ^{6}Li in the positive subsystem due to the Stark effect. The term proportional to the scalar polarizability α_0 was put to zero before diagonalizing the perturbation matrix. The values of the other atomic parameters are given in Table 1 of the paper. The position of the single electric crossing point Ep1 is indicated. Lower picture: Zoom on the two levels crossing at Ep1.

Table 1. Experimental values of atomic constants in ^{6}Li: a, b = hyperfine structure constants, α_0, α_2 scalar, tensorial polarizability, g_J = $2p\ ^2P_{\frac{3}{2}}$ Landé factor, $\hat{g}_I$ = nuclear g-factor (Bohr magnetons)

Symbol	Value	Ref.
a [MHz]	-1.155,	[27]
b [MHz]	-0.1	[27]
α_0 $\left[\text{MHz}/(\text{kV/cm})^2\right]$	0.03163	[28]
α_2 $\left[\text{MHz}/(\text{kV/cm})^2\right]$	$4.06{\cdot}10^{-4}$	[28]
g_J	1.335	[29]
$\hat{g}_I$	$4.47654{\cdot}10^{-4}$	[29]

Table 2. Listing of crossing point data for the positive subsystem in ^{6}Li. The corresponding table for the negative subsystem is obtained by the following changes: 1) the sign of each magnetic field value must be reversed. 2) The sign of each magnetic quantum number labelling the magnetic crossing points Bpn must be reversed. 3) The labels of the electric and the BE-crossing points, which show a Berry phase, must be changed according to Fig. 8 .

Name	B [mT]	E [kV/cm]	ϵ [MHz]	(F, M_F)-(F', M'_F)
Bp1	-0.10335	0.	-0.26564	$(\frac{3}{2},\frac{1}{2})$-$(\frac{5}{2},-\frac{3}{2})$
Bp2	-0.04978	0.	2.34180	$(\frac{1}{2},\frac{1}{2})$-$(\frac{3}{2},-\frac{3}{2})$
Bp3	0.06451	0.	0.05000	$(\frac{3}{2},-\frac{3}{2})$-$(\frac{5}{2},\frac{5}{2})$
Bp4	0.12622	0.	1.77922	$(\frac{3}{2},\frac{1}{2})$-$(\frac{5}{2},\frac{5}{2})$
Bp5	0.23458	0.	-2.23480	$(\frac{3}{2},-\frac{3}{2})$-$(\frac{5}{2},\frac{1}{2})$
Ep1	0.	$\pm$ 51.390	-40.52359	$(\frac{3}{2},\frac{1}{2})$-$(\frac{3}{2},-\frac{3}{2})$
BEp	-0.13029	$\pm$ 127.430	-254.8313	$(\frac{3}{2},\frac{1}{2})$-$(\frac{3}{2},-\frac{3}{2})$

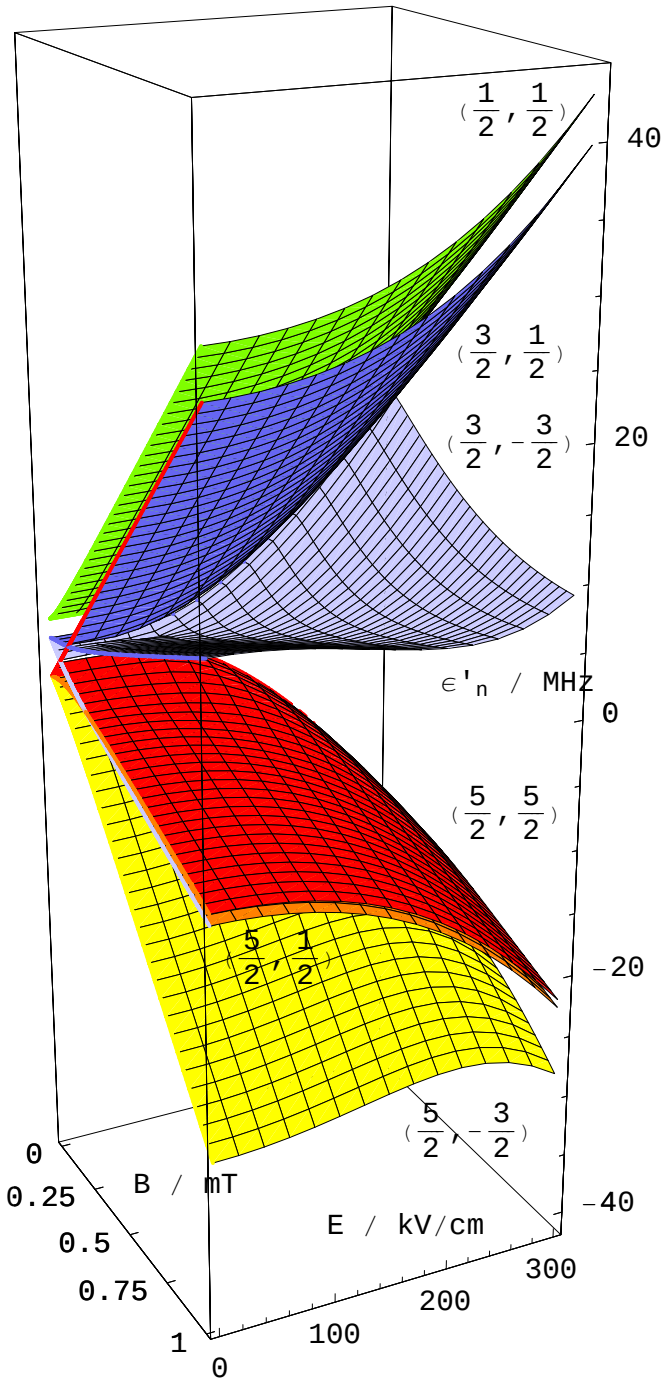

Fig. 3. Energy surfaces in the positive subsystem of ^{6}Li. The magnetic crossing points Bp1, ..., Bp3 are seen on the left.

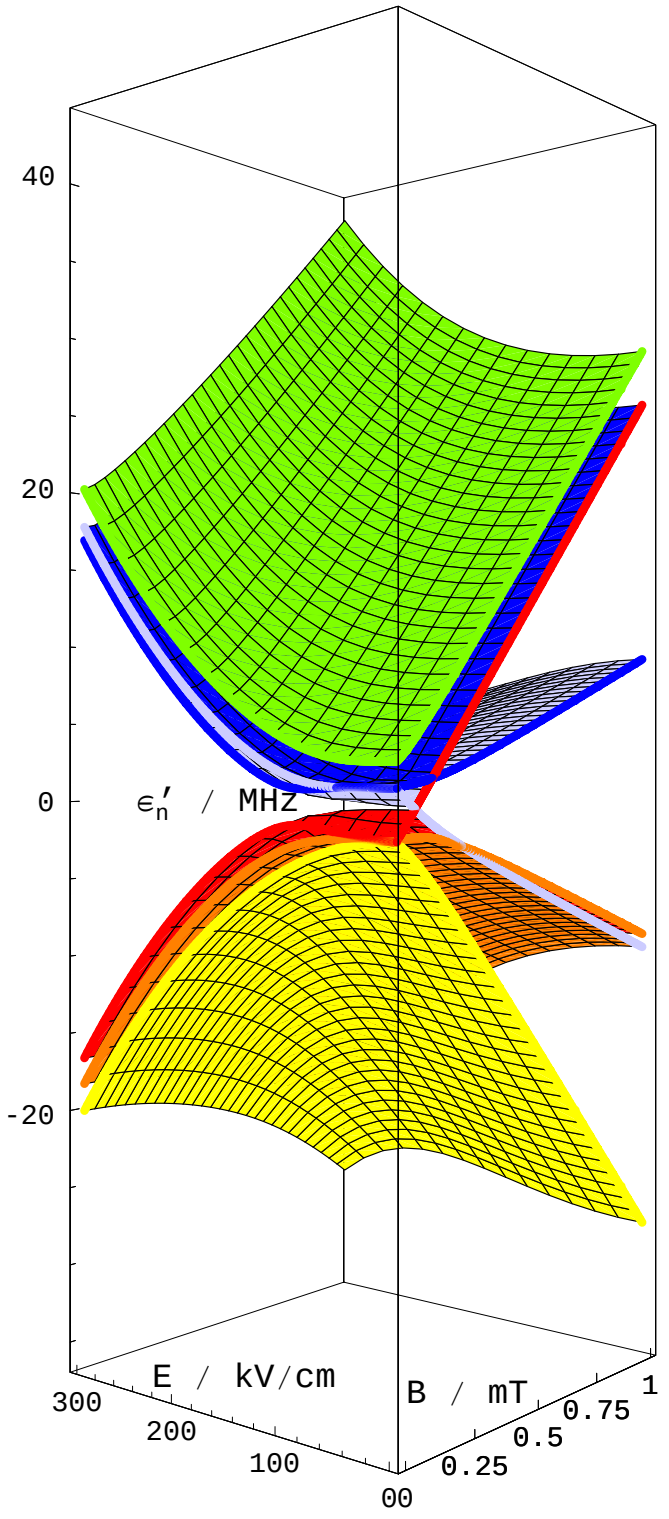

Fig. 4. Energy surfaces in the positive subsystem of ^{6}Li. The electric crossing point Ep1 is seen on the left side, the magnetic crossing points Bp1, ..., Bp3 on the right side.

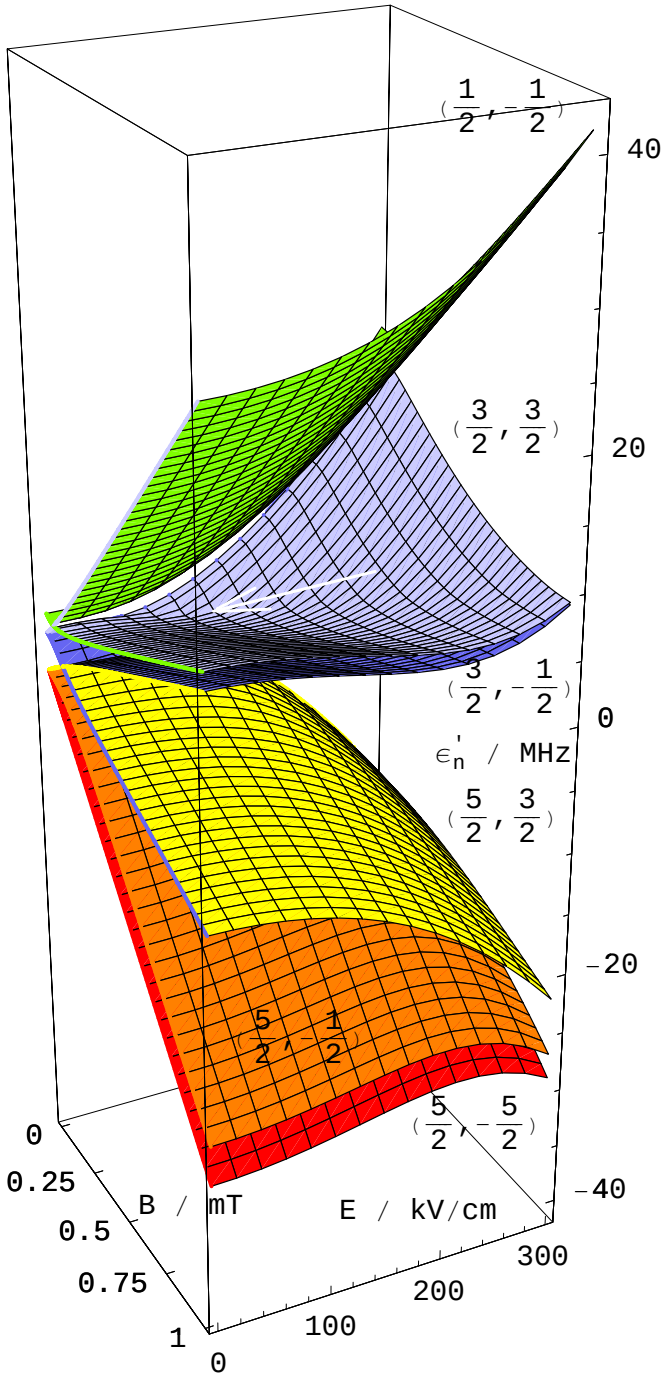

Fig. 5. Energy surfaces in the negative subsystem of ^{6}Li. The magnetic crossing points Bn1 and Bn2 are seen on the left. The arrow points to the crossing point BEn.

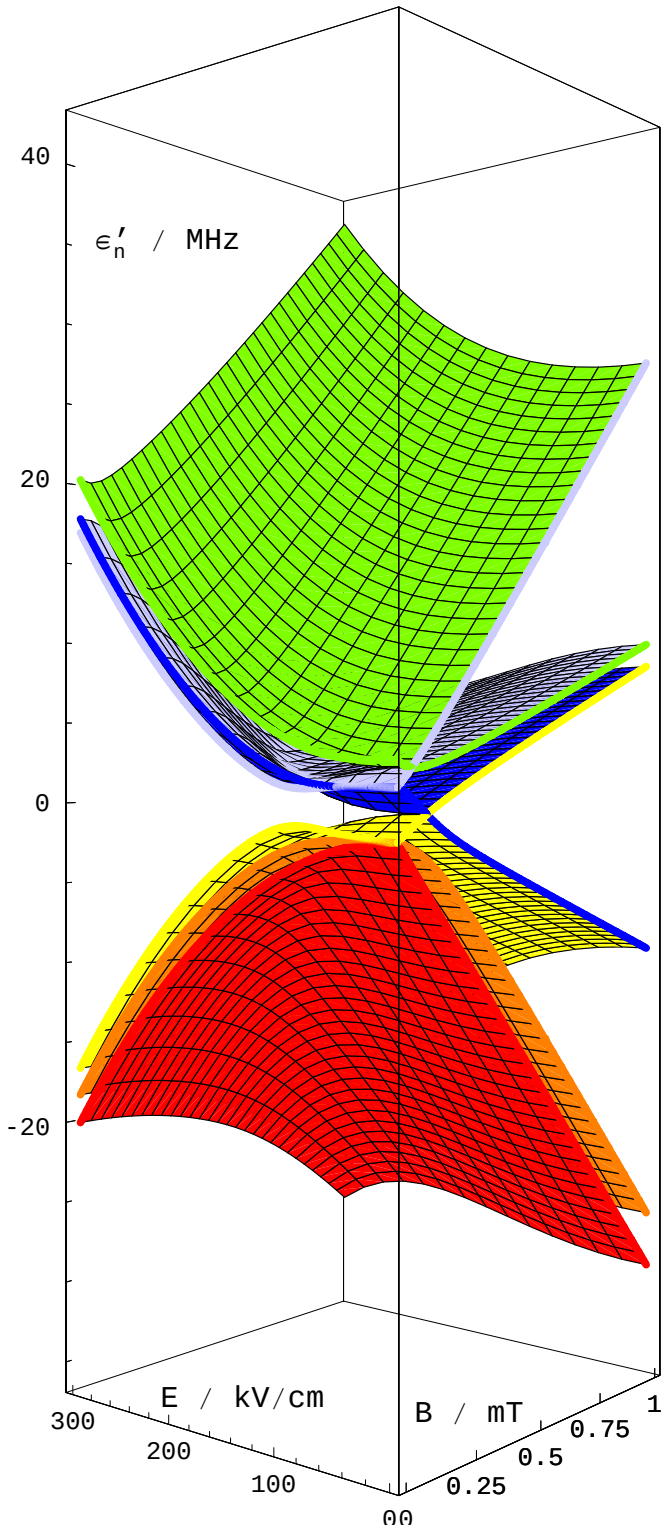

Fig. 6. Energy surfaces in the negative subsystem of ^{6}Li. The magnetic crossing points Bn1 and Bn2 are clearly visible on the right, the electric crossing point En1 on the left.

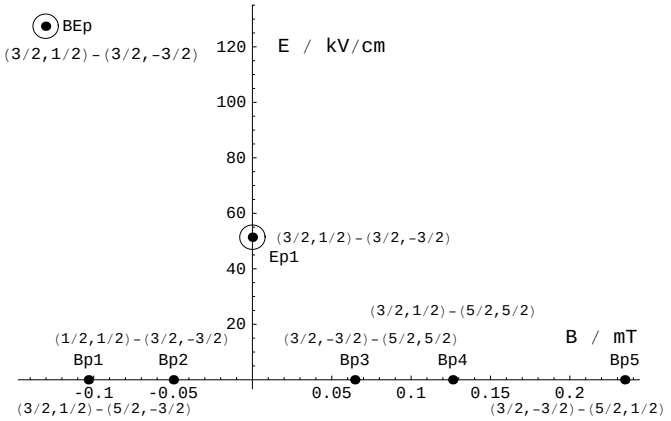

Fig. 7. Crossing diagram of the positive subsystem of ^{6}Li. The crossing points showing a Berry phase are marked by circles. The labels (F, M_F) of the two crossing levels are given at the corresponding crossing point.

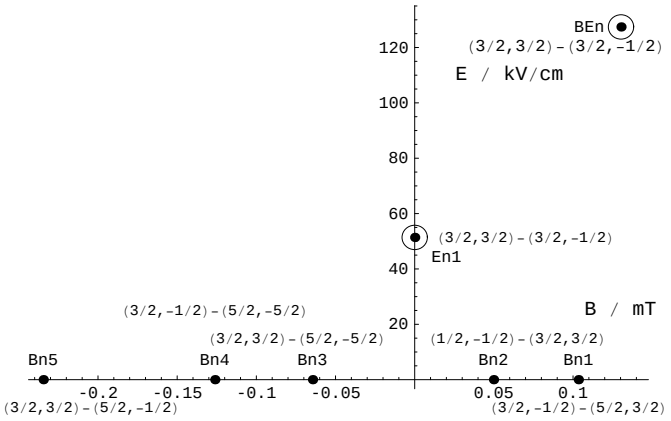

Fig. 8. Crossing diagram of the negative subsystem of ^{6}Li. The crossing points showing a Berry phase are marked by circles. The labels (F, M_F) of the two crossing levels are given at the corresponding crossing point.

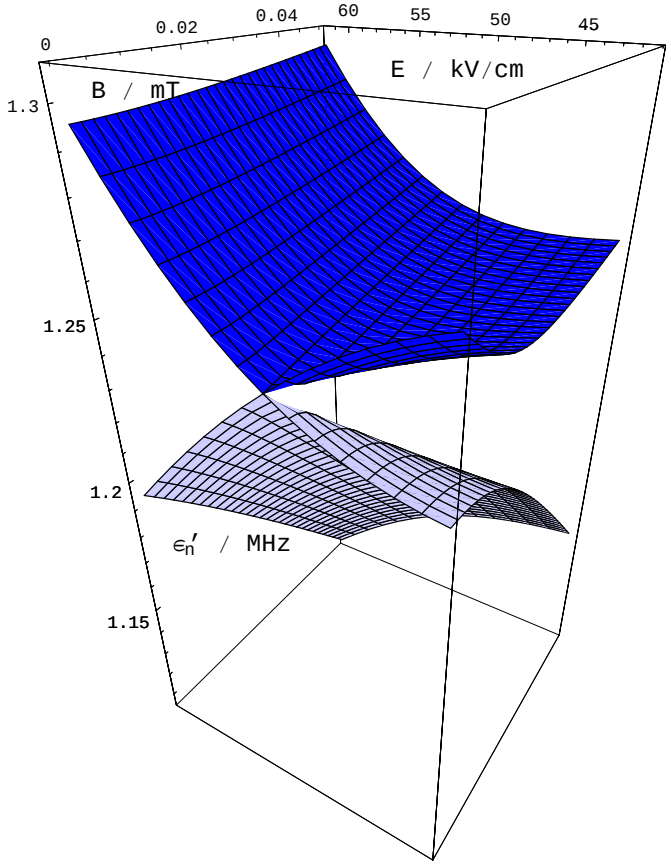

Fig. 9. Energy surface in the neighbourhood of the crossing point $Ep1$, which shows a Berry phase. ϵ'_n is linear in both B and E. The resulting bicone is cut in half in the plane $B = 0$.

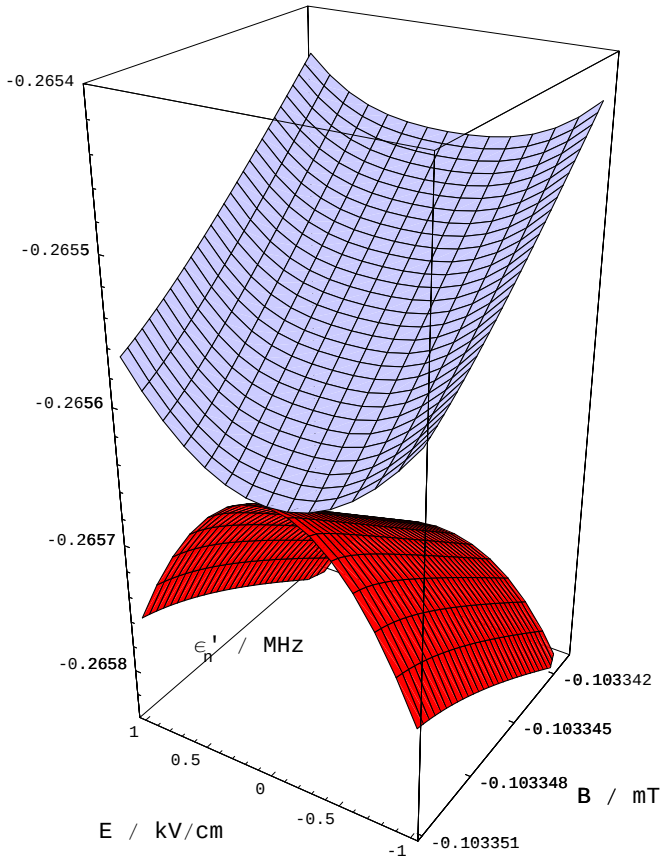

Fig. 10. Energy surfaces in the neighbourhood of the crossing point $Bp1$, which does not show a Berry phase. ϵ'_n is linear in B and quadratic in E. The resulting surfaces are no longer conic sections. They are cut along the plane $B = B_{Bp1} = 0.1033508$ mT.

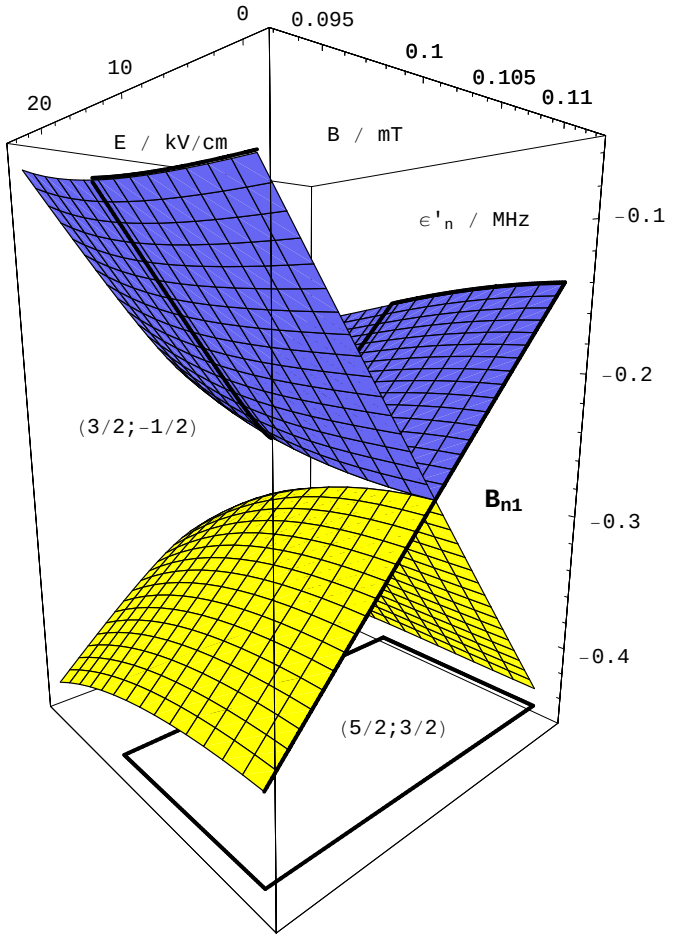

Fig. 11. View of the magnetic crossing point Bn1. The black rectangle at the bottom shows the cycle of fields in the B, E-plane. The black curve gives the corresponding phase curve of the atom on the two parts of the energy surfaces. It starts at $B = 0.093$ mT, $E = 0$ in the surface labelled ($F = 5/2$; $M_F = 3/2$) and ends at the point $B = 0.093$ mT, $E = 0$ on the upper surface with labels ($F = 3/2$; $M_F = -1/2$).

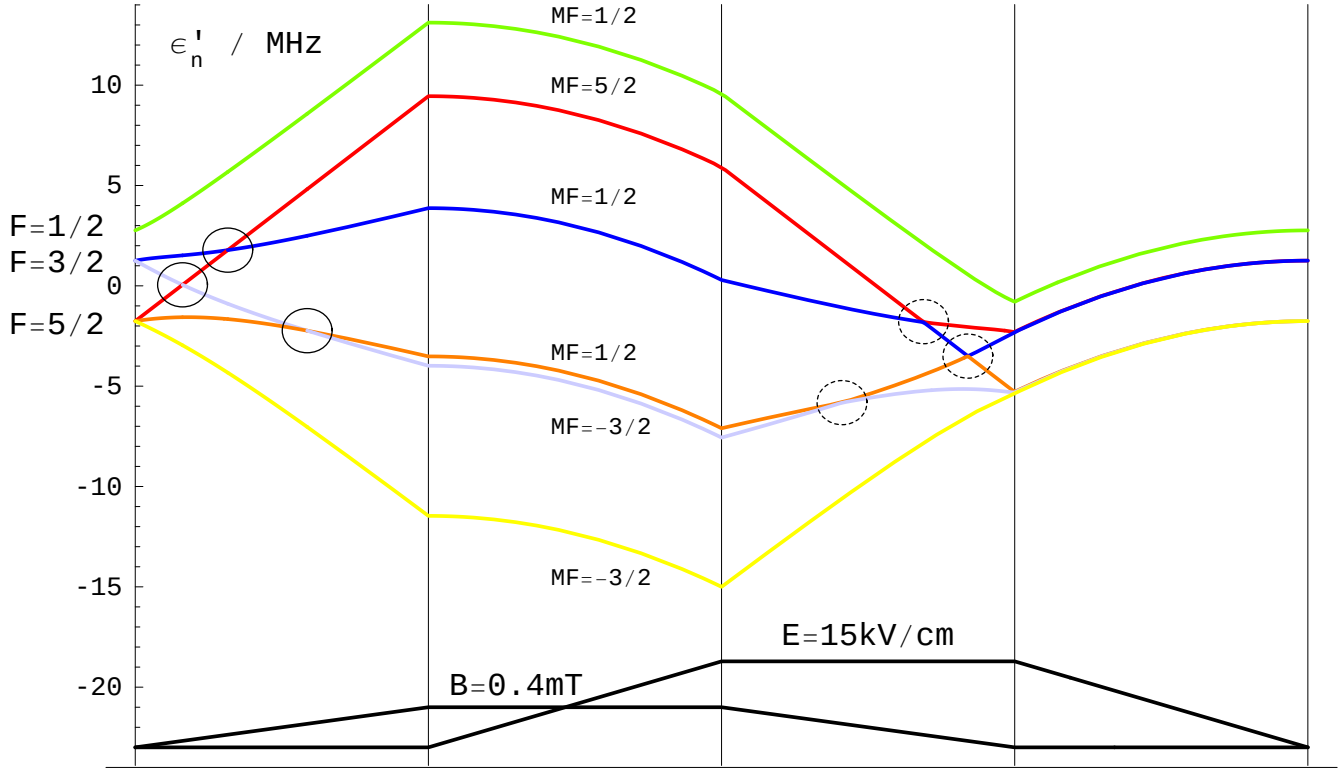
ϵ_n' / MHz
10
5
0
-5
-10
-15
-20
F=1/2
F=3/2
F=5/2
MF=1/2
MF=5/2
MF=1/2
MF=1/2
MF=−3/2
MF=−3/2
E=15kV/cm
B=0.4mT

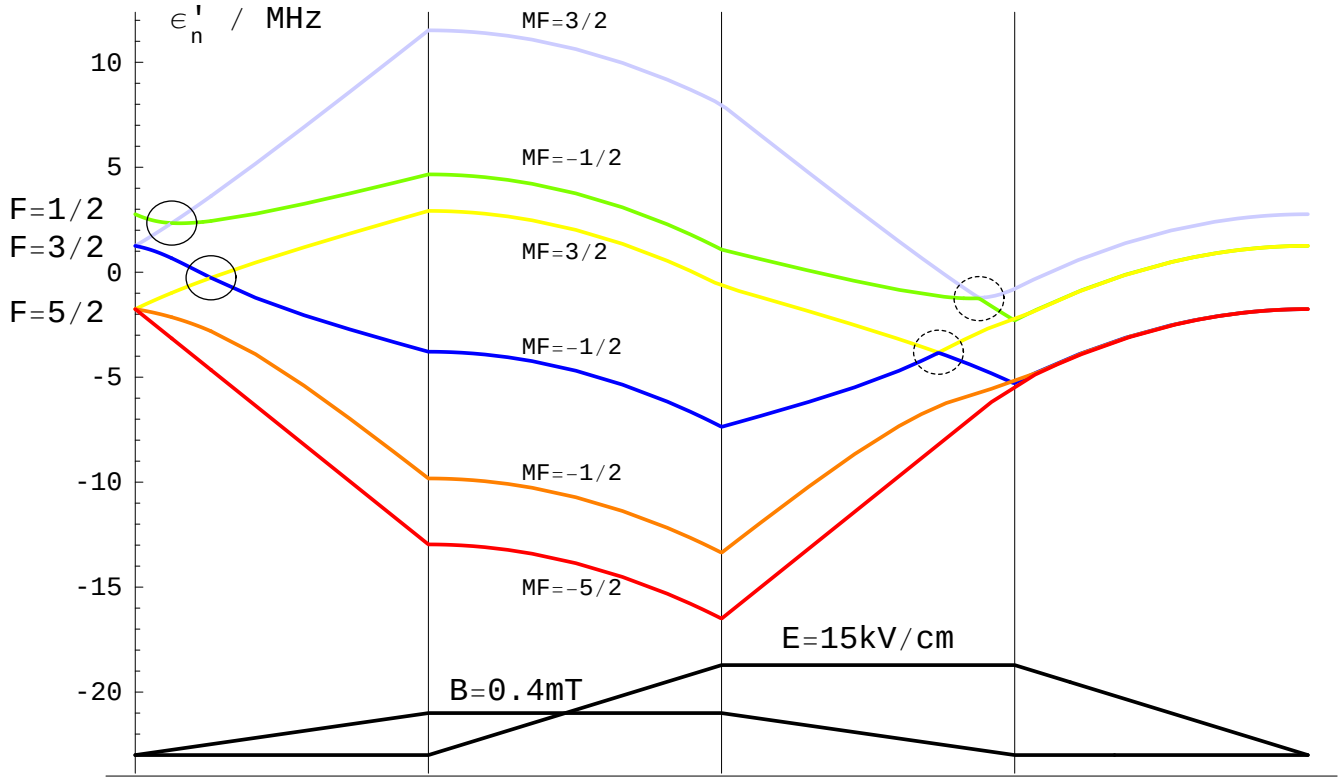

Fig. 12. Upper picture: Sample field cycle of the electromagnetic field with the corresponding splitting of the 2p $^2P_{3/2}$ hyperfine levels of ^{6}Li in the positive subsystem. For lack of space, the magnetic quantum numbers are written in the second interval; they are only valid in the first interval, where there is only a magnetic field present. The total angular momentum numbers F as well as the corresponding magnetic number M_F are assigned to the level and curve by analytic continuation, i.e. according to the overlap of the eigenvectors found by in- or decrementing the field values in sufficiently small steps. There are crossings (anticrossings) within the continuous (dashed) circles.

Lower picture: The same for the negative system.